Adhesion Forces Measured by Atomic Force Microscopy in Humid Air

ARTICLE *in* ANALYTICAL CHEMISTRY · JUNE 2000

Impact Factor: 5.64 · DOI: 10.1021/ac991198c · Source: PubMed

2 AUTHORS, INCLUDING:

Dana Sedin
New Belgium Brewing Company
5 PUBLICATIONS **197** CITATIONS

Anal. Chem. **2000,** *72,* 2183−2189

Articles

Adhesion Forces Measured by Atomic Force Microscopy in Humid Air

Dana L. Sedin and Kathy L. Rowlen*

Department of Chemistry and Biochemistry, University of Colorado, Boulder Colorado 80309

Adhesive forces measured with an atomic force microscope under ambient conditions are generally regarded to be dominated by non-surface-specific capillary force. In this study, the nature of the "pull-off" force on a variety of surfaces was investigated as a function of relative humidity. The results indicate that even under the condition where capillary condensation occurs there is chemical specificity in the measured pull-off force. Issues such as tip−surface contact time and surface roughness were ruled out as possible artifacts. A mathematical model of pull-off force as a function of relative humidity is proposed in which the chemical specificity is explained.

Accurate determination of adhesive forces on the molecular level has led to significant insight in many fields of science.[1−3] Atomic force microscopy (AFM) provides a simple and sensitive (piconewton) means of determining adhesive forces with a high degree of spatial resolution.[2] Numerous forces have been studied by AFM. For example, by modifying AFM tips, colloidal forces,[4] hydrophobic and hydrophilic forces,[5] and chiral forces[6] have been studied. Single bond rupture forces have also been measured by AFM.[7]

Using AFM, adhesive forces are probed by measuring the degree of distortion in a cantilever as the tip is retracted from the surface. Interaction forces can be studied under a wide range of environmental conditions including ambient, vacuum, controlled gas, and liquid. However, due to the large capillary force exerted on the tip in the presence of water vapor, most measurements made with the AFM are conducted under liquid.[4−7] The liquid environment typically yields adhesion forces that are 1 or 2 orders of magnitude less than the same measurements made in humid air.[8]

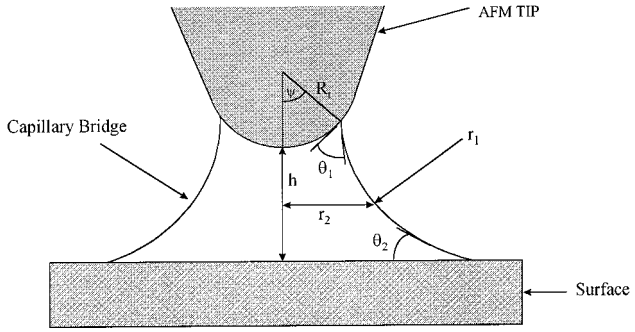

Figure 1. Graphical representation of a capillary bridge formed between an AFM tip and surface. R_t is the radius of curvature for the AFM tip, ψ is the fill angle, r_1 and r_2 are the principal radii of curvature of the meniscus, θ_1 is the contact angle for water on the AFM tip, and θ_2 is the contact angle for water on the surface.

Capillary force results from condensation of water vapor between the surface and AFM tip during contact. When condensation occurs, a capillary bridge (as shown in Figure 1) forms between the tip and surface. Capillary condensation tends to occur on hydrophilic surfaces. The equilibrium radius of the capillary bridge meniscus has long been described by the Kelvin equation:[9,10]

$$\left[\frac{1}{r_1}+\frac{1}{r_1}\right]^{-1} = r_K = \frac{\gamma_L V}{RT\log(p/p_o)} \qquad (1)$$

where r_1 and r_2 are the principal radii of curvature of the meniscus

* To whom correspondence should be addressed: (phone) (303)492−3631; (fax) (303)492−5894; (e-mail) Rowlen@Spot.Colorado.edu.

(1) Craig, V. *Colloids Surf. A* **1997**, *129−130*, 75−93.
(2) Prater, C. B.; Maivald, P. G.; Kjoller, K. J.; Heaton, M. G. Digital Instruments Application Note, 1995.
(3) Capella, B.; Dietler, G. *Surf. Sci. Rep.* **1999**, *34*, 1−105.
(4) Ducker, W. A.; Senden, T. J.; Pashley, R. M. *Nature* **1991**, *353*, 239−241.
(5) Frisbie, C. D.; Rozsnyai, L. F.; Noy, A.; Wrighton, M. S.; Lieber, C. M. *Science* **1994**, *265*, 2071−2074.
(6) McKendry, R.; Theoclitou, M.; Rayment, T.; Abell, C. *Nature* **1998**, *391*, 566−568.
(7) Williams, J. M.; Han, T.; Beebe, T. P. *Langmuir* **1996**, *12*, 1291−1295.
(8) Weisenhorn, A. L.; Hansma, P. K.; Albrecht, T. R.; Quate, C.F. *Appl. Phys. Lett.* **1989**, *26*, 2651−2653.

10.1021/ac991198c CCC: $19.00
Published on Web 04/13/2000

(as shown in Figure 1), r_K is the Kelvin radius, γ_L is the surface tension of the liquid, V is the molar volume of the liquid, R is the gas constant, T is the temperature, and p/p_o is the relative vapor pressure. The Kelvin equation has been experimentally verified for radii as small as 4 nm.[10] Burnham and co-workers estimated a capillary force by calculating the Laplace pressure acting over an area.[11] They approximated the surface area of the meniscus between an AFM tip and a flat surface to be $2\pi R_t h$, where R_t is the radius of the tip and h is the height of the meniscus. The capillary force (F_{cap}) may then be estimated by[11]

$$F_{cap} = 2\pi R_t h \gamma_L / rK \qquad (2)$$

In this expression, F_{cap} is nonsurface specific since its magnitude depends only on the characteristics of the liquid (i.e., γ_L).

Several researchers have investigated the effect of relative humidity on AFM.[12−19] Early on, a study by Hansma and co-workers demonstrated a 100-fold reduction in pull-off forces on mica when the experiment was conducted under liquid water rather than in humid air.[8] That study, combined with the fact that the Kelvin equation is regarded only as "a useful guideline",[20] may account for general statements in the literature that, in the regime of capillary condensation between an AFM tip and the surface, little, if any, chemically specific information can be obtained by pull-off force measurements.[21] While such may be the case for certain surface/tip combinations, this investigation of pull-off forces as a function of relative humidity provides strong evidence to the contrary.

EXPERIMENTAL SECTION

Deflection curves were obtained with a Molecular Imaging PicoSPM in contact mode with an S scanner (6 μm lateral range). Cantilever spring constants were calculated from the resonance frequency of the cantilever.[22] The effect of water vapor adsorption onto the spring constant of the cantilever was regarded as negligible based on work by Thundat and co-workers.[18] Cantilever deflection values were obtained offline using the offline/view/graph subroutine in the Nanoscope software (4.23r2). Adhesive force was calculated by multiplying the appropriate cantilever deflection by its spring constant. The tips used were Si_3N_4 (Digital Instruments NP, 100 μm cantilever length, 20−40 nm radius of curvature, 0.1−0.4 N/m spring constant). Before and after each experiment, the quality of the AFM tip was evaluated by imaging a vapor-deposited silver film (∼5 nm height) on mica. The tip was rejected if artifacts were observed in the silver film image (for example, multiple tip contact points). Force curves were obtained under the following conditions: 1.97 Hz Z scan rate, 512 points collected per line, and the average count set to 1. Contact time was varied by adjusting the Z scan rate. The contact time was calculated by dividing the sample travel distance while the tip is in contact by the average velocity of the sample.

Muscovite mica and highly ordered pyrolitic graphic surfaces were cleaved prior to use. Quartz (ESCO, S1-UVB) and p-doped silicon ⟨111⟩ (Silicon Quest International) were cleaned by sequential sonication (∼5 min) in chloroform (Fisher Scientific, ACS grade), acetone (Fisher Scientific, ACS grade), and methanol (Burdick and Jackson, HPLC grade) or treated in a boiling piranha solution of 70% H_2SO_4 (Mallinckrodt) and 30% H_2O_2 (Fisher, ACS grade) for 15 min. The two different cleaning procedures resulted in different water contact angles on the surfaces. After cleaning, the quartz and silicon surfaces were dried under a flow of USP nitrogen.

The AFM was enclosed in a Molecular Imaging CleanLoad glovebox. Relative humidity within the glovebox was controlled by an adjustable ratio of dry to wet nitrogen (USP). The water used to humidify the chamber was distilled and deionized (18 MΩ). Humidity levels were monitored continuously by a Vaisla RS80 radiosonde. Prior to measurement, the humidity was allowed to reach equilibrium as indicated by a constant value for >3 min. For experiments conducted on two substrates, mica (∼0.5 cm × 1 cm) was glued (Digital Imaging adhesive tabs), or held down using a Molecular Imaging liquid cell, to quartz or silicon (∼1 cm × 1 cm). A polonium source (Static Master, 1c200) was placed over both samples to reduce electrostatic effects between the AFM tip and surface. Surfaces were heated to 100 °C for 1 min, when the relative humidity in the chamber dropped below 10%, to drive off any water from the surface. The samples were not heated for experiments at or above 50% relative humidity. Typically, three force curves were obtained on both samples from approximately 0 to 80% relative humidity, in steps of 5−10%.

Silicon samples were roughened in a solution of NH_4OH (Mallinckrodt)/H_2O (1/5) at 80 °C for varying amounts of time.[23,24] To ensure that SiO_2 was present on the surface of silicon after roughening, the samples were placed in a boiling piranha solution for 15 min.[25,26] The presence of SiO_2 was experimentally verified using a Nicolet Impact 410 FT-IR. Tapping mode AFM images of the roughened silicon surfaces were obtained using a Digital Instruments Nanoscope IIIa (with an E scanner). Etched single-crystal silicon Digital Instruments TESP tips were used. Prior to imaging, the quality of the tip was evaluated by imaging polystyrene nanospheres (50 nm diameter) on mica. The tapping mode imaging conditions were as follows: 1.97 Hz scan rate, 512 points collected per line, and the integral gain and proportional gain both

(9) Israelachvili, J. *Intermolecular and Surface Forces*; Academic Press: London, 1991.
(10) Fisher, L. R.; Israelachvili, J. N. *J. Colloid Interface Sci.* **1981**, *80*, 528−541.
(11) Burnham, N. A.; Colton, R. J.; Pollock, H. M. *J. Vac. Sci. Technol.* **1991**, *9*, 2548−2856.
(12) Fujihira, M.; Aoki, D.; Okabe, Y.; Takano, H.; Hokari, H.; Frommer, J.; Nagatani, Y.; Sakai, F. *Chem. Lett.* **1996**, *7*, 499−500.
(13) Fuji, M.; Machida, K.; Takei, T.; Watanabe, T.; Chikazawa, M. *Langmuir* **1999**, *15*, 4584−4589.
(14) Sugawara, Y.; Ohta, M.; Konishi, T.; Morita, S.; Suzuki, M.; Enomoto, Y. *Wear* **1993**, *168*, 13−16.
(15) Piner, R. D.; Mirkin, C. A. *Langmuir* **1997**, *13*, 6864−6868.
(16) Eastman, T.; Zhu, D. *Langmuir* **1996**, *12*, 2859−2862.
(17) Binggeli, M.; Mate, C. M. *Appl. Phys. Lett.* **1994**, *4*, 415−417.
(18) Thundat, T.; Warmack, R. J.; Chen, G. Y.; Allison, D. P. *Appl. Phys. Lett.* **1994**, *64*, 2894−2896.
(19) Thundat, T.; Zheng, X.-Y.; Chen, G. Y.; Warmack, R. J. *Surf. Sci. Lett.* **1993**, *294*, L939−L943.
(20) Xu, L.; Lio, A.; Hu, J.; Ogletree, D. F.; Salmeron, M. *J. Phys. Chem. B.* **1998**, *102*, 540−548.
(21) Wenzler, L. A.; Moyes, G. L.; Olson, L. G.; Harris, J. M.; Beebe, T. P. *Anal. Chem.* **1997**, *69*, 2855−2861.
(22) Cleveland, J. P.; Manne, S.; Bocek, D.; Hansma, P. K. *Rev. Sci. Instrum.* **1993,** *64*, 403−405.
(23) Utani, K.; Suzuki, T.; Adachi, S. *J. Appl. Phys.* **1993**, *73*, 3467−3471.
(24) Gould, G.; Irene, E. A. *J. Electrochem. Soc.* **1989**, *136*, 1108−1112.
(25) Gurevich, A. B.; Weldon, M. K.; Chabal, Y. J.; Opila, R. L.; Sapjeta, J. *Appl. Phys. Lett.* **1999,** *74*, 1257−1259.
(26) Williams, K. R.; Muller, R. S. *J. Microelectromech. Sys.* **1996**, *5*, 256−269.

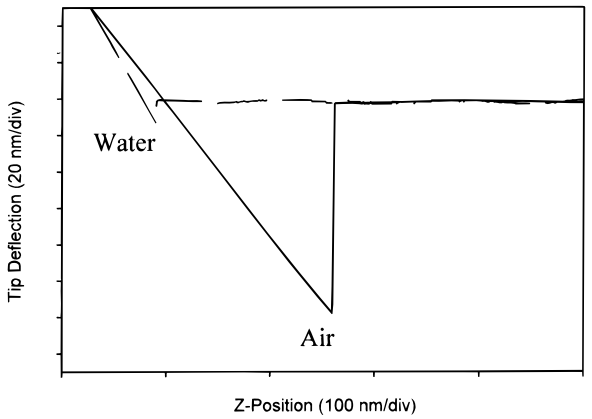

Figure 2. Deflection curves (only retraction) demonstrating the large difference between the pull-off force when measured under water (dashed line) versus under ambient conditions (solid line), ~30% relative humidity, with the same Si_3N_4 tip.

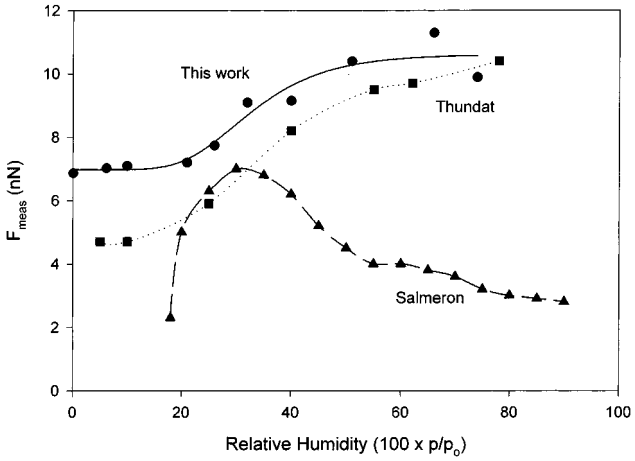

Figure 3. Pull-off force on mica as a function of relative humidity for this work (filled circles), Thundat et al.[19] (filled squares), and Salmeron and co-workers[28] (filled triangles). The lines serve only as viewing aids.

set to 0.6. Surface roughness was evaluated by flattening the images (second order) and calculation of the root-mean-squared (rms) roughness the Nanoscope software (4.23r2).

Contact angle measurements were made with a Leica MZ8 optical microscope (10×−80× magnification) with a digital camera. A 10-μL syringe was used to carefully place a 5 μL water droplet onto the surface of interest. A digital side view image of the droplet was acquired for later processing with PhotoShop software. Contact angles were determined by measuring the angle between the surface and a tangent drawn on the water droplet image. Five measurements were made on each surface.

RESULTS AND DISCUSSION

Adhesive Forces Measured in Air and Water. Figure 2 shows two deflection curves obtained on mica with the same AFM tip, one measured in air and one in water. The *x*-axis of the deflection curve shows the relative distance the sample must be moved away from the tip in order to disengage the tip from the surface. The magnitude of the cantilever deflection during the sample movement is plotted on the *y*-axis. Figure 2 shows that the adhesive force for the AFM tip on mica under water is ~1 order of magnitude less than it is in air. The difference in adhesive force, measured in air compared to water, is not only due to capillary force. The solvent can affect the magnitude of adhesive forces through both solvation and solvent exclusion. It has been shown that the force required to separate a hydrophilic tip and substrate in water is less than the force required to separate a hydrophobic tip and substrate in water, which is directly related to the solvation properties of water.[27]

Pull-Off Force on Mica as a Function of Relative Humidity. To better understand the role of water on the measured pull-off force, a detailed study of adhesive forces as a function of relative humidity was conducted for a variety of surfaces. Representative data are shown in Figure 3 for mica. Figure 3 shows a clear transition point in the pull-off force on mica as a function of relative humidity. Of importance here is the nature of the transition. While others have observed a similar transition point on mica, there is not much agreement on the trend above the transition point, as shown in Figure 3. Thundat et al. observed a flat response in force at relative humidities less than 20%, followed by a pronounced increase which did not level off at humidities up to 80%.[19] They used a model composed of the Lennard-Jones potential and a term for capillary force to fit the trend *above* the transition point. Salmeron and co-workers found a virtually flat response in pull-off force on mica at relative humidities less than 20%, a dramatic transition near 20%, and a maximum at 25−30%, followed by a gradual decrease.[20]

Using scanning polarization force microscopy,[20,28] Salmeron and co-workers probed the structure of the water layer on mica as a function of relative humidity. In early work, the authors described two distinct structural phases of the water film, phase I being an icelike film and phase II a more liquidlike island structure.[20,28] They attributed the transition in pull-off force as a function of relative humidity to the transition from a tightly bound icelike layer of water on mica to more liquidlike islands which lead to capillary condensation during tip contact. In later work, they used a combination of vibrational sum frequency generation and scanning polarization force microscopy and concluded that above the transition point the AFM tip induces water nucleation and therefore the formation of a capillary bridge.[29] Below 20% relative humidity, there is insufficient surface water and no capillary bridge is formed. Interestingly, an ellipsometric study of water on mica as a function of relative humidity indicated no abrupt change in the water layer thickness until near 90% relative humidity.[30] Thus, the transition point in adhesive forces measured by AFM near 20−30% relative humidity is not likely due to the formation of a complete monolayer.

Our hypothesis is that the nature and extent of interaction between water and the surface plays a key role in determining both the magnitude of the adhesive force and the relative humidity where capillary condensation first occurs (i.e., the transition point).

(27) Sinniah, S. K.; Steel, A. B.; Miller, C. J.; Reutt-Robey, J. E. *J Am. Chem. Soc.* **1996**, *118*, 8925−8931.

(28) Hu, J.; Xiao, X.-D.; Ogletree, D. F.; Salmeron, M. *Science* **1995**, *268*, 267−269.

(29) Miranda, P. B.; Xu, L.; Shen, Y. R.; Salmeron, M. *Phys. Rev. Lett.* **1998**, *81*, 5876−5879.

(30) Beaglehole, D.; Christenson, H. K. *J. Phys. Chem.* **1992**, *96*, 3395−3403.

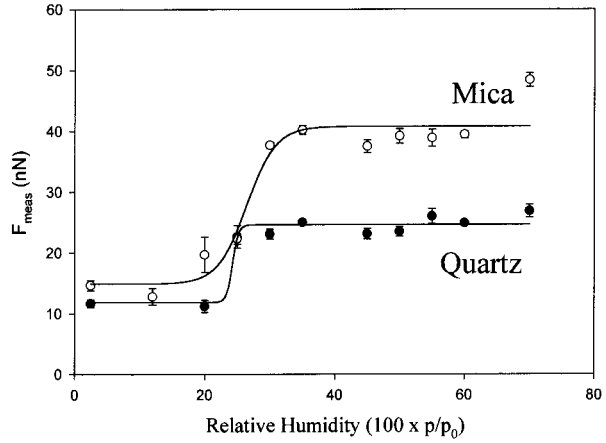

Figure 4. Pull-off force as a function of relative humidity on mica and quartz substrates. For mica the solid line represents nonlinear regression to eq 11. The fit parameters for mica were as follows: $F_{stv} = 15 \pm 2$, $F_{cap} = 26 \pm 3$, $p'/p'_o = 26 \pm 1$, $m = 2.2 \pm 1$, and $r^2 = 0.93$. For quartz, the solid line represents nonlinear regression to eq 11. The fit parameters for quartz were as follows: $F_{stv} = 12 \pm 1$, $F_{cap} = 13 \pm 1$, $p'/p'_o = 24 \pm 63$, $m = 0.4 \pm 38$, and $r^2 = 0.96$. The quartz surface was solvent cleaned (water contact angle 49°).

As a first test of that hypothesis, the pull-off force as a function of relatively humidity was obtained simultaneously for both quartz and mica; data are presented in Figure 4. To compare the magnitude of the pull-off force on different substrates, it is essential that the same tip be used under exactly the same conditions for both surfaces. Direct comparison and intercomparison of pull-off forces in this study were facilitated by using mica as an internal standard. Mica and the other substrate of interest were examined simultaneously. By positioning a small, thin piece of mica on a larger piece of the other substrate, the tip could be moved between mica and the other surface at each relative humidity.

Note in Figure 4 that the pull-off force magnitude is always greater for mica than it is for quartz and that the difference is enhanced at higher relative humidities, reaching a value nearly 2 times that of quartz. In addition, the data in Figure 4 exhibit a clear transition point and the transition for quartz appears to be slightly lower than it is for mica. However, the transition point is not particularly reproducible, as discussed later in the text, probably due to surface contamination. The general trend in pull-off force shown in Figure 4 is reminiscent of a type IV adsorption isotherm described by Brunauer.[31] Type IV isotherms are "considered to reflect capillary condensation phenomena in that they level off before the saturation pressure is reached...".[32] Alternatively, such adsorption isotherms can result from two-dimensional condensation at submonolayer coverages. This "phase transition" at the surface is the result of strong "lateral" interactions between molecules or molecular aggregates.[32]

Proposed Model. It is proposed that at low relative humidity there is insufficient water on the surface to allow for capillary condensation.[20,28−30] In this regime, the tip−surface adhesive force is dictated by interaction in water vapor. At relative humidities higher than the transition point, capillary condensation occurs and the tip−surface adhesive force is the sum of the tip−surface interaction force in liquid water and the capillary force. The proposed form of the relationship between measured pull-off force and relative humidity is

$$F_{meas} = F_{stv} + \frac{F_{stw} + F_{cap}}{1 + e^{-[((p/p_o)-(p'/p'_o))/m]}} \quad (3)$$

where F_{meas} is the measured pull-off force, F_{stv} is the surface−tip adhesive force in the presence of water vapor, F_{stw} is the surface−tip adhesive force in the presence of liquid water, F_{cap} is the adhesive force due to capillary condensation, p/p_o is the relative humidity, p'/p'_o is the relative humidity at the transition point between the two regimes, and m is the slope of the transition. The term F_{stv} may be calculated from the familiar relationship between work and interfacial free energy.[9] The work (W) required to separate unit areas of two solids (subscripts 1 and 2) from contact in the presence of a third substance (such as a vapor or liquid, subscript 3) is defined as

$$W_{132} = \gamma_{13} + \gamma_{23} - \gamma_{12} \quad (4)$$

where γ_{ij} is the interfacial energy for substances i and j. Utilizing the Derjaguin approximation and neglecting JKR theory,[9] the force required to separate two spheres of substances 1 and 2 in the presence of substance 3 is

$$F = 2\pi(R_{s_1}R_{s_2}/(R_{s_1} + R_{s_2}))W_{132} \quad (5)$$

where R is sphere radius. In the case explored here, the tip is approximated by an incompressible sphere with a radius of curvature, R_t, interacting with a hard, flat surface (i.e., where $R_{s_2} \gg R_{s_1}$) such that eq 5 simplies to

$$F = 2\pi R_t W_{132} \quad (6)$$

When the tip and sample are composed of the same material (e.g.,

Table 1. Average Pull-Off Force on Mica, Silicon, Quartz, and HOPG[a]

substrate	F_{meas} (nN)	N	$F_{substrate}/F_{mica}$	measd contact angle
piranha cleaned				
silicon	23 ± 1	27	1.18 ± 0.08	~0
mica	20 ± 1	15		~0
quartz	31 ± 3	27	0.94 ± 0.14	9.2 ± 0.6
mica	33 ± 4	27		~0
HOPG	13 ± 2	15		86[b]
mica	27 ± 1	135	0.48 ± 0.03	~0
solvent cleaned				
silicon	14 ± 1	30	0.79 ± 0.05	25 ± 1
mica	17 ± 1	30		~0
quartz	21 ± 1	63	0.69 ± 0.05	49 ± 1
mica	30 ± 2	63		~0

[a] Standard error of the mean is reported for the experiments. The pull-off force for HOPG was not measured with mica in the same experiment; all of the pull-off force experiments on mica were averaged for comparison. F_{meas}, average pull-off force above 50% relative humidity. N, number of measurements. [b] Reference 37

(31) Brunauer, S. *The Adsorption Of Gases and Vapors;* Princeton University Press: London, 1943.

(32) Adamson, A. *Physical Chemistry of Surfaces*; John Wiley & Sons: New York, 1976.

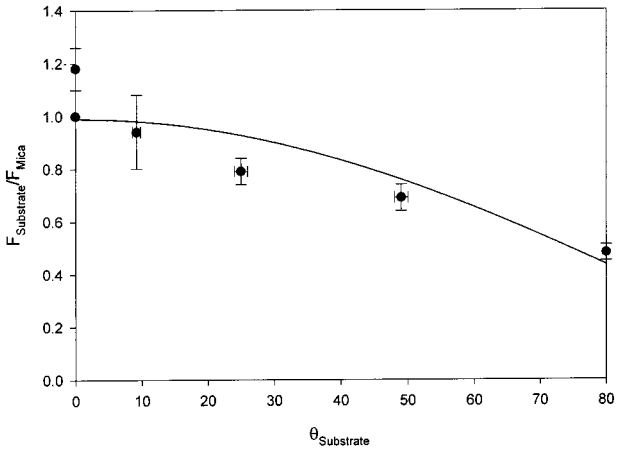

Figure 5. Ratio of pull-off forces ($F_{substrate}/F_{mica}$) plotted as a function of the water contact angle on the various substrates. While it is not possible to fit the data, since the fill angle is not necessarily a constant, the solid line shows the qualitative relationship between F_{cap} and θ_2. Specifically, H (eq 10) is plotted against θ_2 reasonably assuming that $r_2 \gg r_1$.[9]

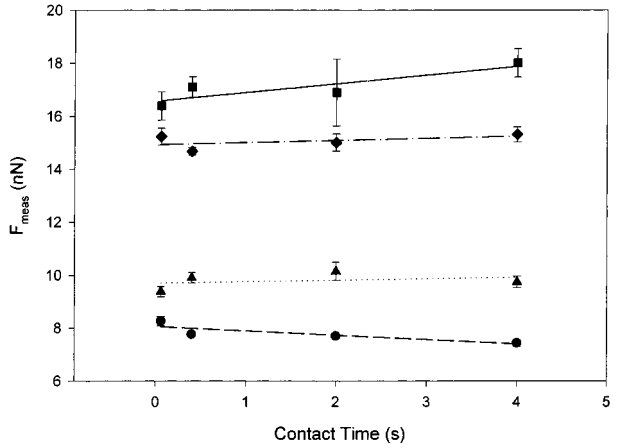

Figure 6. Pull-off force on mica as a function of tip−mica contact time. The dashed line (filled circles) is a linear fit to data taken at 5% relative humidity (slope -0.17 ± 0.07). The dotted line (filled triangles) is a linear fit to data taken at 24% relative humidity (slope 0.0054 ± 0.12). The dashed and dotted line (filled diamonds) is a linear fit to data taken at 75% relative humidity (slope 0.08 ± 0.09). The solid line (filled squares) is a linear fit to data taken at 46% relative humidity (slope 0.33 ± 0.13).

SiO_2), the expression simplifies to

$$F_{stv} = 4\pi R_t \gamma_{sv} \qquad (7)$$

where γ_{sv} is the surface interfacial free energy in vapor (water vapor in this case).

Evaluation. As an order of magnitude estimate of F_{stv} for a SiO_2-terminated tip interacting with a quartz surface in water vapor (i.e., the regime before the onset of capillary condensation), the surface free energy of SiO_2 in water vapor (γ_{13} ~100 mJ/m^2)[33] and a R_t of 10 nm was used. Equation 7 predicts an adhesive force of 12−13 nN, which is in good agreement with the value determined by fitting the data shown in Figure 4 to eq 3 (~12 nN). From four separate experiments on quartz, the value of F_{stv} obtained from nonlinear regression to eq 3 ranged from ~5 to ~12 nN (the average correlation coefficient for the fit was 0.98). As an order of magnitude estimate for a SiO_2-terminated tip (R_t of 10 nm) interacting with a mica surface in vapor, the surface free energy of SiO_2 in water vapor (γ_{13} ~100 mJ/m^2), the free energy for mica in water vapor (γ_{23} ~300 mJ/m^2),[9] and an *estimated* van der Waals interfacial energy (γ_{12}) of ~50 mJ/m^2[9] was used in eq 4. Equation 6 then yields a calculated adhesive force of ~22−23 nN, which is higher than the value obtained from a fit of the data shown in Figure 4 (~15 nN). From 10 separate experiments conducted on mica over a two-month time period, the value of F_{stv} obtained from fitting the data to eq 3 ranged from ~5 to ~15 nN (the average correlation coefficient for the nonlinear regressions was 0.96). It is not possible to average F_{stv} for all of

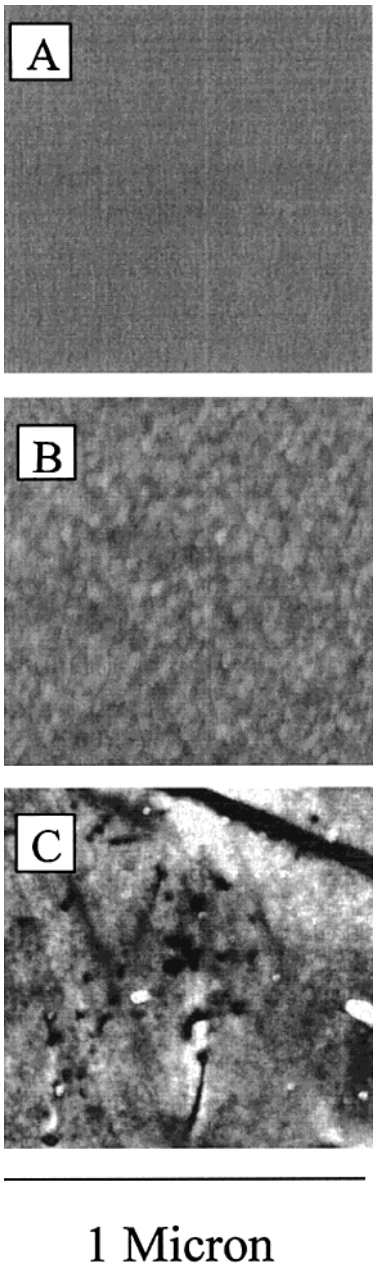

Figure 7. Tapping mode 1 μm × 1 μm images of mica (A), silicon (B), and quartz (C). The image rms roughness for mica is 0.03 nm, for silicon is 0.13 nm, and for quartz is 0.87 nm. Lighter shades are taller features with the z-scale being 2 nm.

(33) Janczuk, B.; Zdziennicka, A. *J. Mater. Sci.* **1994**, *29*, 3559−3564.

Table 2. Pull-Off Force as a Function of Silicon Roughness[a]

substrate		immersion time (s)	rms roughness 500 nm	rms roughness 1000 nm	rms roughness 5000 nm	F_{meas}[b]
(A)[c]	silicon	0	0.15 ± 0.06	0.14 ± 0.01	0.17 ± 0.02	23 ± 1
	mica					20 ± 1
(B)[d]	silicon	150	1.8 ± 0.5	2.3 ± 0.02	3.8 ± 1.8	23 ± 1 (25 ± 1) [34 ± 3]
	mica					20 ± 2 (26 ± 1) [31 ± 1]
(C)[e]	silicon	300	2.9 ± 1.2	2.3 ± 1.1	3.8 ± 0.4	23 ± 2 (19 ± 1) [24 ± 3]
	mica					25 ± 1 (25 ± 1) [19 ± 1]

[a] The range from two separate samples is reported for the rms roughness values. Standard error of the mean is reported for the pull-off force. [b] F_{meas}, average pull-off force above 50% relative humidity. [c] This data set consists of two separate experiments over a 5 month period. [d] Data in parentheses and brackets are from two additional data sets with silicon roughened for 150 s, in which the rms roughness of the surfaces was not quantified. The three data sets were taken over a five-month period. [e] Data in parentheses and brackets are from two additional data sets with silicon roughened for 255 s, in which the rms roughness of the surfaces was not quantified. The three data sets were taken over a five-month period.

the experiments since the pull-off force is dependent on the tip shape and size, both of which are known only qualitatively.

The value for F_{stw} is difficult to determine due to the number of unknowns. However, it is likely that the capillary force dominates the numerator in the second term of eq 3. Although not generally discussed within the atomic force microscopy literature, the total capillary force may be calculated as the sum of the surface tension (F_t) and the force due to a pressure difference across a sphere's surface (F_p). Orr et al.[34] use the following approach:

$$F_t = 2\pi R_t \gamma_w \sin(\psi) \sin(\psi + \theta_1) \quad (8)$$

$$F_p = -2\pi H \gamma_w R_t^2 \sin^2(\psi) \quad (9)$$

where R_t is the radius of curvature of the spherical tip, γ_w is the interfacial free energy water, ψ is the filling angle, θ_1 is the contact angle for water on the sphere, and H is the local mean curvature as is defined for a circle approximation of the meniscus:[34]

$$H = \left(\frac{1}{r_1} + \frac{1}{r_2}\right) = \frac{1}{2R_t}\left[-\left(\frac{\cos(\theta_1 + \psi) + \cos(\theta_2)}{1 - \cos(\psi)}\right) + \frac{\sin(\theta_1 + \psi)}{\sin(\psi)}\right] \quad (10)$$

where θ_2 is the contact angle for water on the flat surface and r_1, r_2 are defined in Figure 1. Several researchers have used a similar approach to calculate the total capillary force exerted between a sphere and a flat surface.[35,36]

Thus, if we reasonably assume that $F_{cap} \gg F_{stw}$, eq 3 may be written

$$F_{meas} \approx F_{stv} + \frac{F_t + F_p}{1 + e^{((p/p_o) - (p'/p'_o))/m}} \quad (11)$$

The important implication of eqs 3 and 11 is that the adhesive force in the regime where capillary condensation clearly dominates is *surface specific*. The measured pull-off force depends on the contact angle for water on the surface. It is further hypothesized that for scrupulously clean surfaces the transition point (p'/p'_o) and slope of the transition (m) are both related to the nature of water−surface interaction. A nonlinear regression of the data shown in Figure 4 to eq 11 (or equivalently eq 3) yields a value for F_{cap} (i.e., $F_t + F_p$) of ∼26 and ∼13 nN for mica and quartz, respectively. On the basis of 10 separate experiments on mica, F_{cap} ranged from ∼ 4 to 26 nN. On the basis of four separate experiments on quartz, F_{cap} ranged from 4 to ∼ 13 nN. The transition point (p'/p'_o) for mica ranged from ∼18 to 36% relative humidity and the transition point for quart from 24 to 50% relative humidity. The broad range is likely due to surface contamination (despite the precautions taken) as well as tip size/shape.

Adhesive Forces Measured above 50% Relative Humidity. Our study indicates that the pull-off force at relative humidities greater than 50% is essentially constant. To facilitate comparison of a large number of data sets, measurements of pull-off force above 50% relative humidity were averaged for each surface and the ratio of that value to the average value on mica calculated. Table 1 is a summary of the average adhesive forces and contact angles. Comparison of these values provides further evidence that the pull-off force measured in the capillary condensation regime does indeed provide chemically specific information about the surface. For example, Figure 5 is a plot of $F_{substrate}/F_{mica}$ as a function of the water contact angle on the substrate. The substrates were mica, quartz, silicon, and highly ordered pyrolytic graphite. The solid line in Figure 5 shows the qualitative behavior of F_{cap} as a function of the water contact angle on the substrate (θ_2). As demonstrated in both Table 1 and Figure 5, both the water contact angle and the pull-off force are sensitive to surface contamination. Use of piranha solution as the surface cleaning agent, rather than a sequential solvent rinse, results in a significant change in the water contact angle and measured pull-off force. As expected, solvents appear to leave behind organic contaminants while piranha cleaning is known to remove organics from silicon surfaces.[26]

Tip−Sample Contact Time. There is some evidence that the measured pull-off force in humid air is affected by the contact time between the tip and surface.[20] To rule out such effects as

(34) Orr, F. M.; Scriven, L. E.; Rivas, A. P. *J. Fluid Mech.* **1975**, *67*, 723−742.
(35) de Lazzer, A.; Dreyer, M.; Rath, H. J. *Langmuir* **1999**, *15*, 4551−4559.
(36) Marmur, A. *Langmuir* **1993**, *9*, 1922−1926.
(37) Drzymala, J. *Adv. Colloid Interface Sci.* **1994**, *50*, 143−185.

the source of surface specificity, the pull-off force on mica was measured as a function of both relative humidity and tip−surface contact time. Figure 6 is a plot of pull-off force as a function of contact time for 5, 24, 46, and 75% relative humidity. The contact time between the AFM tip and sample was adjusted from milliseconds (typical contact time in AFM experiments) to 4 s. Linear regression was used to fit each data set and the slope and error in the slope were extracted for each line. The slopes are identical within error (as shown in the caption for Figure 6).

Surface Roughness. Another potential source of measured differences in pull-off force for a variety of surfaces is surface roughness, especially if the contact area between the tip and surface is significantly different. The surface roughness varies substantially for the four substrates investigated (mica, graphite, quartz, silicon). For example, Figure 7 shows 1 μm × 1 μm top view images of mica (A), silicon (B), and quartz (C) obtained by tapping mode AFM. To evaluate the influence of roughness on the measured pull-off force, silicon surfaces were chemically roughened in NH_4OH_{aq}. Ammonium hydroxide solutions are known to etch both SiO_2 and Si surfaces.[23,24] To maintain the same surface chemistry for a variety of roughness values, the silicon was chemically oxidized in piranha after etching.[25,26] The presence of an SiO_2 layer was verified by FT-IR. Table 2 contains a summary of measured roughness as a function of immersion time in NH_4OH_{aq}. As is clear from the measured pull-off forces as a function of immersion time in Table 2, within error, relatively large differences in surface roughness did not significantly affect the measurement.

ACKNOWLEDGMENT

The authors gratefully acknowledge funding from the National Science Foundation.

Received for review October 18, 1999. Accepted January 28, 2000.

AC991198C